

CHAOS ASSOCIATED WITH FLUID INERTIA.

K. BAJER* & H.K. MOFFATT **

Institute for Theoretical Physics

University of California

Santa-Barbara, California 93106-4090, U.S.A.

ABSTRACT. The low Reynolds number flow between two concentric steadily rotating spheres is considered. The pattern of streamlines is explained in terms of an adiabatic invariant. It is shown that, when the two rotation vectors are not parallel, the streamlines become chaotic when the Reynolds number Re is increased and the onset of global chaos occurs near $Re = 20$.

1. Introduction

The objective of this work is to determine whether, and to what extent, fluid inertia is responsible for the presence of chaos, and associated particle dispersion, in the streamlines of steady flow of an incompressible fluid. In a parallel study (Bajer & Moffatt 1990, Bajer, Moffatt & Nex, 1990) it has been shown that a wide family of inertialess (Stokes) flows in a spherical domain are characterised by chaotic streamlines; however these flows can be generated only by appropriate, and rather artificial, conditions imposed on the tangential velocity at the boundary, and would be difficult to realise in practise. Stone, Nadim & Strogatz (1991) have studied similar Stokes flows inside a spherical droplet immersed in a general linear flow. Such flows have chaotic streamlines and are possible to realise in practice. The problem of the flow inside a droplet is similar to the problem of the electromagnetic stirring of molten metals (Moffatt, 1991). High frequency external magnetic fields together with the shape of the domain occupied by liquid metal determine the velocity components tangent to the surface of the domain. There exists a unique Stokes flow compatible with this imposed surface velocity, but in metallurgical applications the Reynolds number is, usually, high and

* Permanent address: University of Warsaw, Institute of Geophysics, ul. Pasteura 7, 02-093 Warszawa, Poland

** Permanent address: DAMTP, University of Cambridge, Silver Street, Cambridge CB3 9EW, UK.

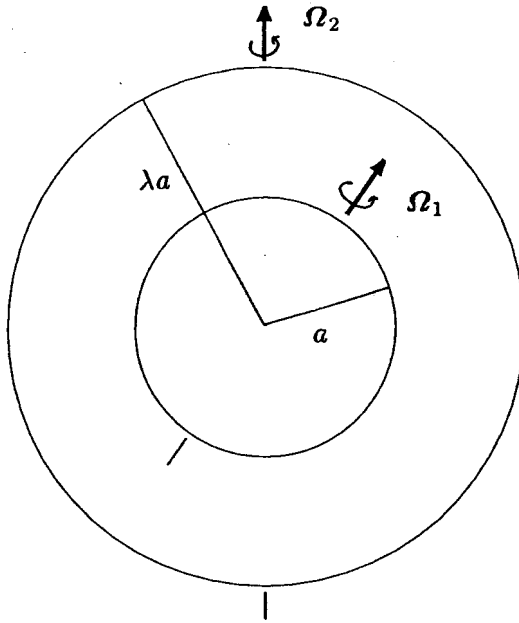


Fig. 1. The domain of the flow - spherical annulus between two concentric solid spheres rotating steadily.

fluid inertia is important. The flow that we consider in this paper is easily realisable. In the Stokes limit, in which inertia is neglected, it has closed streamlines. The question that we address is: what happens to the streamline pattern when account is taken of fluid inertia, even when this is weak in relation to viscous effects.

Specifically, we consider the flow in the spherical annulus between two concentric spheres of radii a , λa ($\lambda > 1$), rotating with angular velocities Ω_1 , Ω_2 respectively (figure 1). In the Stokes regime, the solution to this problem is well-known (Landau & Lifshitz, 1987, p.65): the steady velocity field $\mathbf{u}^{(0)}(\mathbf{x})$ driven by viscous stresses alone is given by

$$\mathbf{u}^{(0)}(\mathbf{x}) = f_1(r)\Omega_1 \wedge \mathbf{x} + f_2(r)\Omega_2 \wedge \mathbf{x}, \quad (1.1)$$

where r is distance from the centre measured in units of a (i.e. $1 < r < \lambda$ in the annulus), and

$$f_1(r) = \frac{(\lambda/r)^3 - 1}{\lambda^3 - 1}, \quad f_2(r) = \frac{\lambda^3 - (\lambda/r)^3}{\lambda^3 - 1} = 1 - f_1(r) \quad (1.2)$$

The flow (1.1) satisfies the condition $\mathbf{x} \cdot \mathbf{u}^{(0)}$, i.e. it is a purely *toroidal* flow, and may be expressed in the form

$$\mathbf{u}^{(0)} = \nabla \wedge (\mathbf{x}T^{(0)}(\mathbf{x})) \quad (1.3)$$

where

$$T^{(0)}(\mathbf{x}) = (f_1(r)\Omega_1 + f_2(r)\Omega_2) \cdot \mathbf{x} \quad , \quad (1.4)$$

the streamlines of the flow being given by the intersections of the surfaces $T^{(0)} = cst.$ with spheres $r = cst.$ These streamlines are circles, the circles on a sphere of radius r all lying in planes with normal parallel to the vector $f_1(r)\Omega_1 + f_2(r)\Omega_2$. This vector varies continuously as a function of r from Ω_1 on $r = 1$ to Ω_2 on $r = \lambda$. Obviously the Stokes flow (1.3) has no simple symmetry, and it may be expected that this simple streamline pattern may be severely disrupted when account is taken of inertia.

In section 2 we calculate the secondary flow induced by the rotation of only one sphere, while a general formula for arbitrary Ω_1 and Ω_2 is given in section 3. In order to understand the pattern of streamlines in the limit $Re = \Omega_1 a^2/\nu \rightarrow 0$ we derive an equation for the adiabatic drift (section 4) and consider the influence of the departures from axisymmetry on the drift surfaces (section 5).

2. Secondary flow associated with rotation of one sphere

It is a straightforward matter to calculate the secondary flow $\mathbf{u}^{(1)}(\mathbf{x})$ driven by (weak) inertia forces when only one of the spheres rotates. Specifically, suppose that $\Omega_1 \neq 0$, $\Omega_2 = 0$. Then the resulting flow will be axisymmetric about the direction of Ω_1 . Let (r, θ, φ) be spherical polar coordinates based on this axis of symmetry, and let $\psi^{(1)}(r, \theta)$ be the Stokes streamfunction of the secondary flow in the meridian plane; then the streamlines of the composite flow $\mathbf{u}^{(0)} + \mathbf{u}^{(1)}$ will be helices wound on the family of nested tori $\psi^{(1)}(r, \theta) = cst.$ (figure 2), the helicity being antisymmetric about the plane $\theta = \pi/2$.

With $\mathbf{u}^{(0)}(\mathbf{x}) = f_1(r)\Omega_1 \wedge \mathbf{x}$ the convective (centrifugal) acceleration associated with $\mathbf{u}^{(0)}$ is

$$\begin{aligned} \mathbf{u}^{(0)} \cdot \nabla \mathbf{u}^{(0)} &= f_1(r)(\Omega_1 \wedge \mathbf{x}) \cdot \nabla \{f_1(r)\Omega_1 \wedge \mathbf{x}\} \\ &= f_1^2(r)[(\mathbf{x} \cdot \Omega_1)\Omega_1 - \Omega_1^2 \mathbf{x}], \end{aligned} \quad (2.1)$$

and the curl of this quantity, which is responsible for the generation of vorticity in the secondary flow, is given by

$$\begin{aligned} \nabla \wedge \{\mathbf{u}^{(0)} \cdot \nabla \mathbf{u}^{(0)}\} &= (\mathbf{x} \cdot \Omega_1)G_{11}(r)(\mathbf{x} \wedge \Omega_1) \\ &= -\frac{1}{2}\nabla \wedge \{(\Omega_1 \cdot \mathbf{x})^2 G_{11}(r)\mathbf{x}\} \end{aligned} \quad (2.2)$$

where

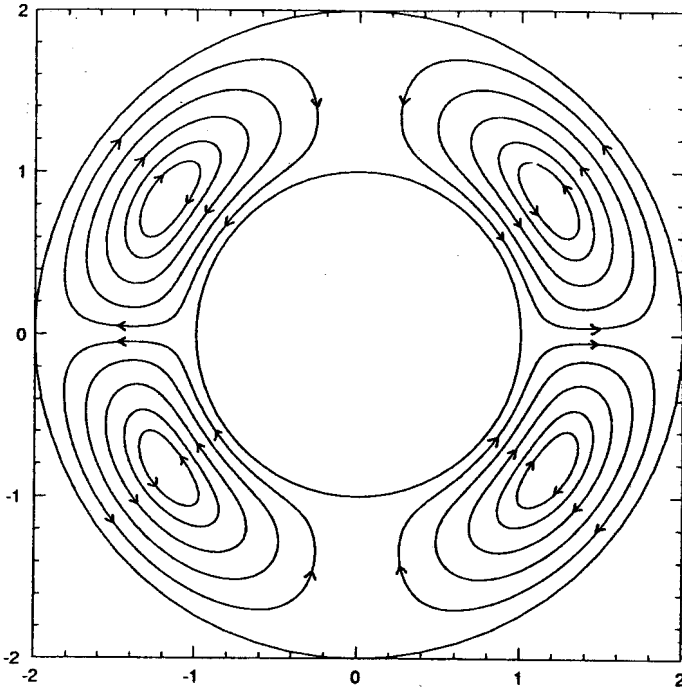


Fig. 2. Surfaces of constant $\Psi^{(1)}$ for $\Omega_1 = 1$, $\Omega_2 = 0$, $\lambda = 2$.

$$G_{11}(r) = 2r^{-1} f_1(r) f_1'(r) = \frac{6\lambda^3(1 - (\lambda/r)^3)}{(\lambda^3 - 1)^2 r^5}. \quad (2.3)$$

The vorticity field $\omega^{(1)} = \nabla \wedge \mathbf{u}^{(1)}$ driven by (2.2) is toroidal in character; this means that, as expected, $\mathbf{u}^{(1)}$ is poloidal (i.e. meridional in this axisymmetric situation). Writing $\mathbf{u}^{(1)}$ in the form

$$\mathbf{u}^{(1)} = \nabla \wedge \nabla \wedge (\mathbf{x} P^{(1)}(\mathbf{x})) \quad (2.4)$$

we have

$$\omega^{(1)} = \nabla \wedge \mathbf{u}^{(1)} = -\nabla \wedge (\mathbf{x} \nabla^2 P^{(1)}). \quad (2.5)$$

Note that $P^{(1)}$ and $\psi^{(1)}$ are related by

$$\psi^{(1)}(r, \theta) = r \sin \theta \frac{\partial P^{(1)}}{\partial \theta}. \quad (2.6)$$

Moreover

$$\nabla^2 \omega^{(1)} = -\nabla \wedge (\nabla \wedge \omega^{(1)}) = -\nabla \wedge (\mathbf{x} \nabla^4 P^{(1)}), \quad (2.7)$$

Now, to first order in the Reynolds number Re , $\omega^{(1)}$ satisfies the equation

$$\nabla^2 \omega^{(1)} = \nu^{-1} \nabla \wedge (\mathbf{u}^{(0)} \cdot \nabla \mathbf{u}^{(0)}) \quad , \quad (2.8)$$

where ν is the kinematic viscosity of the fluid. Comparison of (2.3) and (2.7) then provides the equation for $P^{(1)}$:

$$\nabla^4 P^{(1)} = -\frac{1}{2} \nu^{-1} (\Omega_1 \cdot \mathbf{x})^2 G_{11}(r) + F(r) \quad . \quad (2.9)$$

where $F(\cdot)$ is an arbitrary function. The no-slip boundary conditions are satisfied provided

$$P^{(1)} = 0 \quad , \quad \partial P^{(1)} / \partial r = 0 \quad \text{on} \quad r = 1, \lambda \quad . \quad (2.10)$$

The required solution has the form

$$P^{(1)}(\mathbf{x}) = \alpha(r) (\Omega_1 \cdot \mathbf{x})^2 + \beta(r) \Omega_1^2 \quad (2.11)$$

and then from (2.6),

$$\psi^{(1)}(r, \theta) = 2\Omega_1^2 r \alpha(r) \cos \theta \sin^2 \theta \quad . \quad (2.12)$$

Substitution of (2.11) in (2.9) leads to a fourth-order equation for $\alpha(r)$, namely

$$\left\{ \frac{1}{r^6} \frac{d}{dr} r^6 \frac{d}{dr} \right\}^2 \alpha(r) = -\frac{1}{2\nu} G_{11}(r) \quad . \quad (2.13)$$

It is straightforward, but tedious, to find the solution of this equation ($G_{11}(r)$ being given by 2.3), with boundary conditions (from 2.10)

$$\alpha = 0 \quad , \quad \partial \alpha / \partial r = 0 \quad \text{on} \quad r = 1, \lambda \quad . \quad (2.14)$$

Figure 2 shows the surfaces of constant $\Psi^{(1)}$ for $\Omega_1 = \hat{\mathbf{i}}_z$, $\Omega_2 = 0$, $\lambda = 2$.

3. Spheres spinning around different axes

Let us now consider $\Omega_1 \neq \Omega_2$. The Stokes flow (1.1) is no longer axisymmetric and the curl of the convective acceleration (which is not centrifugal) takes form:

$$\begin{aligned} \nabla \wedge (\mathbf{u}^{(0)} \cdot \nabla \mathbf{u}^{(0)}) &= \nabla \wedge (\mathbf{u}^{(0)} \wedge \omega^{(0)}) \quad (3.1) \\ &= \nabla \wedge \left\{ \left[\frac{(f_1^2)'}{2r} (\Omega_1 \cdot \mathbf{x})^2 + \frac{(f_2^2)'}{2r} (\Omega_2 \cdot \mathbf{x})^2 + \frac{(f_1 f_2)'}{r} (\Omega_1 \cdot \mathbf{x})(\Omega_2 \cdot \mathbf{x}) \right] \mathbf{x} \right\} \end{aligned}$$

The equation for $P^{(1)}$, analogous to (2.9, 2.10) becomes:

$$\nabla^4 P^{(1)} = \frac{(f_1^2)'}{2r} (\Omega_1 \cdot \mathbf{x})^2 + \frac{(f_2^2)'}{2r} (\Omega_2 \cdot \mathbf{x})^2 + \frac{(f_1 f_2)'}{r} (\Omega_1 \cdot \mathbf{x})(\Omega_2 \cdot \mathbf{x}) + F(r)$$

$$P^{(1)} = 0, \quad \frac{\partial P^{(1)}}{\partial r} = 0 \quad \text{on } r = 1, \lambda \quad (3.2)$$

In spherical geometry this double-harmonic equation can be solved by a general procedure of expanding $P^{(1)}$ and the right-hand side in a series of spherical harmonics. With an appropriate choice of $F(\cdot)$ the solution is:

$$P^{(1)} = \frac{3}{(\lambda^{-3} - 1)^2} \left[\alpha_1(r)(\Omega_1 \cdot \mathbf{x})^2 + \alpha_2(r)(\Omega_2 \cdot \mathbf{x})^2 + \alpha_3(r)(\Omega_1 \cdot \mathbf{x})(\Omega_2 \cdot \mathbf{x}) \right],$$

where α_i satisfy the following ODEs:

$$(\hat{O}_6)^2 \alpha_1(r) = -\frac{1}{r^8} + \frac{\lambda^{-3}}{r^5} \quad (3.3a)$$

$$(\hat{O}_6)^2 \alpha_2(r) = -\frac{1}{r^8} + \frac{1}{r^5} \quad (3.3b)$$

$$(\hat{O}_6)^2 \alpha_3(r) = +\frac{2}{r^8} - \frac{1 + \lambda^{-3}}{r^5} \quad (3.3c)$$

$$\alpha_i(1) = \alpha_i(\lambda) = \alpha_i'(1) = \alpha_i'(\lambda) = 0 \quad (3.3d)$$

$$\hat{O}_6 = \frac{1}{r^6} \frac{d}{dr} r^6 \frac{d}{dr} \quad (3.4)$$

A general solution of (3.3) takes form:

$$\alpha_i = \frac{(r-1)^2(r-\lambda)^2}{r^5} \left[C_i^0 + C_i^1 r + C_i^2 r^2 + C_i^3 r^3 \right] \quad (3.5)$$

and the coefficients C_i^j are determined by the boundary conditions. Finally we obtain the following expression for $P^{(1)}$:

$$P^{(1)} = L(\lambda)R(r, \lambda) \sum_{i,j=1}^2 \sum_{k=0}^3 W_{ij}^k(\lambda) r^k (\Omega_i \cdot \mathbf{x})(\Omega_j \cdot \mathbf{x}) \quad (3.6)$$

where:

$$L(\lambda) = \frac{-\frac{1}{8}\lambda^3(\lambda^3 - 1)^{-2}}{4\lambda^6 + 16\lambda^5 + 40\lambda^4 + 55\lambda^3 + 40\lambda^2 + 16\lambda + 4} \quad (3.7)$$

$$R(r, \lambda) = \frac{(r-1)^2(r-\lambda)^2}{r^5} \quad (3.8)$$

$$W_{11}^0(\lambda) = 2\lambda^7 + 8\lambda^6 + 20\lambda^5 + 16\lambda^4 + \lambda^3 - 2\lambda^2 \quad (3.9)$$

$$W_{11}^1(\lambda) = 4\lambda^6 + 16\lambda^5 + 17\lambda^4 - 6\lambda^3 - 18\lambda^2 - 8\lambda$$

$$W_{11}^2(\lambda) = 2(1 + \lambda)(3\lambda^4 + 2\lambda^3 - 5\lambda^2 - 8\lambda - 2)$$

$$W_{11}^3(\lambda) = 3\lambda^4 + 2\lambda^3 - 5\lambda^2 - 8\lambda - 2$$

$$W_{22}^0(\lambda) = -2\lambda^7 + \lambda^6 + 16\lambda^5 + 20\lambda^4 + 8\lambda^3 + 2\lambda^2$$

$$W_{22}^1(\lambda) = -8\lambda^7 - 18\lambda^6 - 6\lambda^5 + 17\lambda^4 + 16\lambda^3 + 4\lambda^2$$

$$W_{22}^2(\lambda) = 2(1 + \lambda)\lambda^2(-2\lambda^4 - 8\lambda^3 - 5\lambda^2 + 2\lambda + 3)$$

$$W_{22}^3(\lambda) = \lambda^2(-2\lambda^4 - 8\lambda^3 - 5\lambda^2 + 2\lambda + 3)$$

$$W_{12}^0(\lambda) = W_{21}^0(\lambda) = -\frac{1}{2}\lambda^3(9\lambda^3 + 36\lambda^2 + 36\lambda + 9)$$

$$W_{12}^1(\lambda) = W_{21}^1(\lambda) = -\lambda(-4\lambda^6 - 7\lambda^5 + 5\lambda^4 + 17\lambda^3 + 5\lambda^2 - 7\lambda - 4)$$

$$W_{12}^2(\lambda) = W_{21}^2(\lambda) = 2(1 + \lambda)(\lambda^6 + 4\lambda^5 + \lambda^4 - 2\lambda^3 + \lambda^2 + 4\lambda + 1)$$

$$W_{12}^3(\lambda) = W_{21}^3(\lambda) = \lambda^6 + 4\lambda^5 + \lambda^4 - 2\lambda^3 + \lambda^2 + 4\lambda + 1$$

When $\Omega_1 = \Omega_2$ the flow in a spherical annulus is a solid body rotation. It is then an exact solution of the Navier-Stokes equation, and hence the secondary flow (and the higher order corrections) vanish identically. This implies the following identity:

$$\sum_{i,j=1}^2 W_{ij}^k(\lambda) = 0 \quad \text{for all } \lambda ; \quad (3.10)$$

which can be verified directly from (3.9).

Substituting (3.6) into (2.4) we finally obtain an expression for the secondary flow:

$$\mathbf{u}_1 = A\Omega_1 + B\Omega_2 - C\mathbf{x} , \quad (3.11)$$

$$A = (3C_{11} + r^2D_{11})(\Omega_1 \cdot \mathbf{x}) + (3C_{12} + r^2D_{12})(\Omega_2 \cdot \mathbf{x}) ,$$

$$B = (3C_{12} + r^2D_{12})(\Omega_1 \cdot \mathbf{x}) + (3C_{22} + r^2D_{22})(\Omega_2 \cdot \mathbf{x}) ,$$

$$C = D_{11}(\Omega_1 \cdot \mathbf{x})^2 + 2D_{12}(\Omega_1 \cdot \mathbf{x})(\Omega_2 \cdot \mathbf{x}) + D_{22}(\Omega_2 \cdot \mathbf{x})^2 + C_{11}\Omega_1^2 + 2C_{12}\Omega_1 \cdot \Omega_2 + C_{22}\Omega_2^2 ;$$

where C_{ij} , D_{ij} are functions of r and λ :

$$C_{ij} = 2LR \sum_{k=0}^3 W_{ij}^k r^k , \quad (3.12a)$$

$$D_{ij} = 2L \left[r^{-1} \frac{dR}{dr} \sum_{k=0}^3 W_{ij}^k r^k + \frac{R}{r^{-2}} \sum_{k=0}^3 k W_{ij}^k r^k \right] ; \quad (3.12b)$$

which satisfy an identity analogous to (3.10):

$$\sum_{i,j=1}^2 C_{ij} = \sum_{i,j=1}^2 D_{ij} = 0 . \quad (3.13)$$

When Ω_1, Ω_2 are parallel, for example when

$$\Omega_1 = \omega_1 \hat{i}_z , \quad \Omega_2 = \omega_2 \hat{i}_z , \quad (3.14)$$

we obtain:

$$P^{(1)} = L(\lambda) R(r, \lambda) r^2 \cos^2 \theta \sum_{i,j=1}^2 \sum_{k=0}^3 W_{ij}^k(\lambda) r^k \omega_i \omega_j \quad (3.15)$$

The streamlines of $\mathbf{u}^{(0)} + Re\mathbf{u}^{(1)}$ lie on the surfaces of constant $\Psi^{(1)}$, which can be easily derived from (2.6). The double sum in (3.15) is a cubic polynomial in r . For $\omega_2/\omega_1 \in I = [-0.641, -0.251]$ one of its roots satisfies $1 \leq r_* \leq 2$. Then the secondary flow given by $\Psi^{(1)}$ is a 'two-cell' flow (figure 3), while for $\omega_2/\omega_1 \notin I$ it is a 'single-cell' flow similar to that in figure 2. In particular $\omega_1 = -\omega_2$ is the latter case.

The situation when $(\omega_2 - \omega_1)/\omega_1 \ll 1$ and $Re \gg 1$ was considered by Proudman (1956); in this limit the flow is dominated by Coriolis forces and the structure is determined by boundary layers and internal shear layers. This limit is quite different from the flow considered here.

4. Adiabatic invariants associated with a weak secondary flow

When the streamlines of the basic flow are closed loops, then a small perturbation $\mathbf{u}^{(1)}$ typically causes a drift across closed orbits (Bajer & Moffatt, 1990). The drift is slow compared with the periods of the unperturbed orbits. Every fluid particle, drifting slowly, 'selects' a 1-parameter family of unperturbed orbits, i.e. it outlines a two-dimensional surface¹. In our case a basic (Stokes) flow is given by (1.1) and its (closed) streamlines are determined by two invariants:

$$I_1 = \Omega(r) \cdot \mathbf{x} = \text{const.} , \quad I_2 = r^2 = \mathbf{x}^2 = \text{const.} ; \quad (4.1)$$

¹ In the vicinity of stagnation points the time-scale of an unperturbed flow is infinite. Hence, for any perturbation $\mathbf{u}^{(1)}$ of finite magnitude there exists a small neighbourhood of the stagnation points where the surfaces do not exist

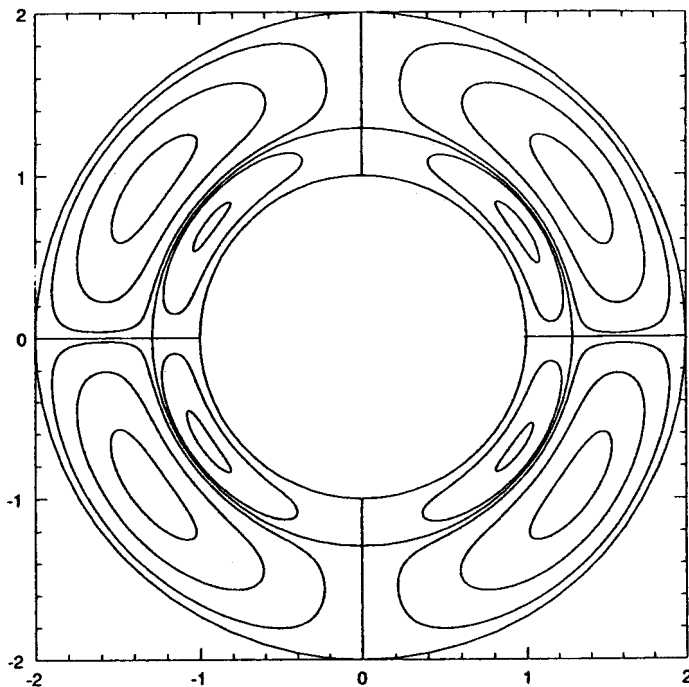


Fig. 3. The axisymmetric 'two-cell' flow.

$$\boldsymbol{\Omega} = f_1(r)\boldsymbol{\Omega}_1 + f_2(r)\boldsymbol{\Omega}_2 \quad .$$

For small Reynolds number the secondary flow (3.11) acts as a small perturbation and the invariants I_1 , I_2 change slowly as a result of an adiabatic drift:

$$\left\langle \frac{dI_1}{dt} \right\rangle = Re \left\{ r^{-1} \frac{df_1}{dr} (\boldsymbol{\Omega}_1 - \boldsymbol{\Omega}_2) \cdot \langle \mathbf{x}(\mathbf{x} \cdot \mathbf{u}^{(1)}) \rangle + \langle \boldsymbol{\Omega} \cdot \mathbf{u}^{(1)} \rangle \right\}, \quad (4.2a)$$

$$\left\langle \frac{dI_2}{dt} \right\rangle = 2Re \left\{ \langle A\boldsymbol{\Omega}_1 \cdot \mathbf{x} \rangle + \langle B\boldsymbol{\Omega}_2 \cdot \mathbf{x} \rangle - \langle C \rangle r^2 \right\}. \quad (4.2b)$$

The angular brackets denote the average over an unperturbed streamline:

$$\mathbf{x}_u(t) = I_1 \boldsymbol{\Omega}^{-1} \hat{\mathbf{k}} + \sigma \cos(\Omega t) \hat{\mathbf{i}} + \sigma \sin(\Omega t) (\hat{\mathbf{k}} \wedge \hat{\mathbf{i}}), \quad (4.3)$$

$$\sigma = \sqrt{I_2 - I_1^2 / \Omega^2} \quad , \quad \hat{\mathbf{k}} = \boldsymbol{\Omega} / \Omega \quad ;$$

where $\hat{\mathbf{i}}$ is any unit vector perpendicular to $\boldsymbol{\Omega}$.

Evaluating these averages we obtain the equations of the slow drift:

$$\frac{1}{Re} \frac{dI_1}{dt} = F_1(I_2)I_1^3 + F_2(I_2)I_1 \quad , \quad (4.4a)$$

$$\frac{1}{Re} \frac{dI_2}{dt} = G_1(I_2)I_1^2 + G_2(I_2) \quad ; \quad (4.4b)$$

with the following functions F_1, F_2, G_1, G_2 :

$$F_1(I_2) = \frac{3df_1/dr}{2\sqrt{I_2}\Omega^3} \sum_{i,j=1}^2 \left\{ C_{ij}[5p_i p_j - \Omega_i \cdot \Omega_j] \hat{k} - p_i \Omega_j - p_j \Omega_i \right\} \cdot (\Omega_1 - \Omega_2) - \frac{1}{2\Omega^2} \sum_{i,j=1}^2 \{ D_{ij}[3p_i p_j - \Omega_i \cdot \Omega_j] \} \quad ,$$

$$F_2(I_2) = \frac{-\sqrt{I_2}}{2\Omega} \sum_{i,j=1}^2 \left\{ C_{ij}[9p_i p_j - \Omega_i \cdot \Omega_j] \hat{k} - 3p_i \Omega_j - 3p_j \Omega_i \right\} \cdot (\Omega_1 - \Omega_2) + \sum_{i,j=1}^2 \{ [C_{ij} + \frac{1}{2}I_2 D_{ij}][3p_i p_j - \Omega_i \cdot \Omega_j] \} \quad ,$$

$$G_1(I_2) = \frac{3}{\Omega^2} \sum_{i,j=1}^2 C_{ij}[3p_i p_j - \Omega_i \cdot \Omega_j] \quad ,$$

$$G_2(I_2) = -\frac{1}{3}I_2\Omega^2 G_1(I_2) \quad ,$$

$$p_i = \hat{k} \cdot \Omega_i \quad .$$

The two-dimensional, autonomous system (4.4) is integrable and its first integral is an adiabatic invariant of the flow $\mathbf{u}^{(0)} + Re\mathbf{u}^{(1)}$.

5. Departures from axisymmetry

When $\Omega_1 \parallel \Omega_2$ the flow is axisymmetric and has one or two 'cells' in each quadrant, depending on ω_2/ω_1 . Now suppose the angle between the directions of Ω_1 and Ω_2 is small but finite. We shall demonstrate that the topology of the stream-surfaces undergoes a discontinuous change in the limit of $\epsilon \rightarrow 0$. Let us first consider two different small perturbations of a simple case $\Omega_1 = \Omega_2$ ($\mathbf{u}^{(1)} = 0$). We take:

a) an axisymmetric perturbation,

$$\Omega_1 = (1 - \epsilon)\hat{\mathbf{i}}_z \quad , \quad \Omega_2 = (1 + \epsilon)\hat{\mathbf{i}}_z \quad ; \quad (5.1a)$$

b) a non-axisymmetric perturbation,

$$\Omega_1 = \epsilon\hat{\mathbf{i}}_z + (1 - \frac{1}{2}\epsilon^2)\hat{\mathbf{i}}_z \quad , \quad \Omega_2 = \hat{\mathbf{i}}_z \quad ; \quad (5.1b)$$

and examine the radial component of the slow drift (see 4.4b):

$$\begin{aligned}
 r^{-1} \langle \mathbf{u}^{(1)} \cdot \mathbf{x} \rangle &= \frac{Re}{2r} (I_1^2 - \frac{1}{3} I_2 \Omega^2) G_1(I_2) \\
 &= \frac{3Re}{r\Omega^4} L(\lambda) R(r, \lambda) S(\mathbf{x}) \quad , \quad (5.2) \\
 S(\mathbf{x}) &= \sum_{i,j=1}^2 \sum_{k=0}^2 W_{ij}^k [3(\Omega_i \cdot \Omega)(\Omega_j \cdot \Omega) - \Omega_i \cdot \Omega_j \Omega^2] r^k \quad .
 \end{aligned}$$

Using (3.10) we obtain the following expressions for $S(\mathbf{x})$:

$$\text{a) } S(\mathbf{x}) = 8\epsilon \sum_{k=0}^3 [(f_1 - 1)W_{11}^k + f_1 W_{22}^k] r^k + O(\epsilon^2) \quad , \quad (5.3a)$$

$$\text{b) } S(\mathbf{x}) = \epsilon^2 \sum_{k=0}^3 [(3f_1 - 2)W_{11}^k + (1 - 3f_1)W_{22}^k] r^k + O(\epsilon^4) \quad (5.3b)$$

Taking, for example, $\lambda = 2$ one can easily verify that in case a) the leading order term in $S(\mathbf{x})$ has no zeros in the interval $1 \leq r \leq \lambda$. In the case b) there is one root $r_0(\lambda)$ for every λ , and $r_0(2) = 1.25259689\dots$

This means that a small axisymmetric departure from $\Omega_1 = \Omega_2$ results in a 'one-cell flow', while a non-axisymmetric deflection of type b) yields two cells with the helicities of opposite sign. In the latter case the boundary between the two cells is at $r = r_0$ when $\epsilon \rightarrow 0$.

The surfaces of constant adiabatic invariant (or drift surfaces) can be obtained by numerical integration of (4.4), see figure 4. The periods of the orbits of $\mathbf{u}^{(0)}$ are bounded. Hence, for small Re the streamlines of $\mathbf{u}^{(0)} + Re\mathbf{u}^{(1)}$ lie on the drift surfaces.

The above analysis shows a discontinuous change of the drift *pattern*, but $\mathbf{u}^{(1)} \equiv 0$ when $\Omega_1 = \Omega_2$, so the *drift* changes continuously in the limit $\epsilon \rightarrow 0$. Considering a small non-axisymmetric departure from $\Omega_1 = (1 - \delta)\Omega_2$, $\delta \ll 1$, we find a continuous change of the drift pattern. As the angle between Ω_1 and Ω_2 tends to zero, one of the two cells in each quadrant disappear into the inner (outer) boundary when $\delta > 0$ ($\delta < 0$).

So far we discussed only the case of Ω_1 and Ω_2 being (nearly) parallel. When $|\Omega_1| = |\Omega_2|$ and the angle α between Ω_1 and Ω_2 is increased the inner and the outer cells change their relative position. Figure 5 shows the drift surfaces for $\alpha = 45^\circ$. If Ω_1 and Ω_2 are anti-parallel, then a small departure from axial symmetry leads to an 'almost discontinuous' change of the drift flow. When $\Omega_1 = -\Omega_2$ the flow $\mathbf{u}^{(0)} + Re\mathbf{u}^{(1)}$ has one cell in each quadrant (see sec. 3). Yet, as can be easily verified, $\langle \mathbf{u}^{(1)} \cdot \mathbf{x} \rangle = 0$ on a spherical surface $r = r_1$ where r_1 is such that $\Omega(r_1) = f_1 \Omega_1 + f_2 \Omega_2 = (1 - 2f_1)\Omega_2 = 0$. This is a special surface where $\mathbf{u}^{(0)} = 0$, i.e. where the

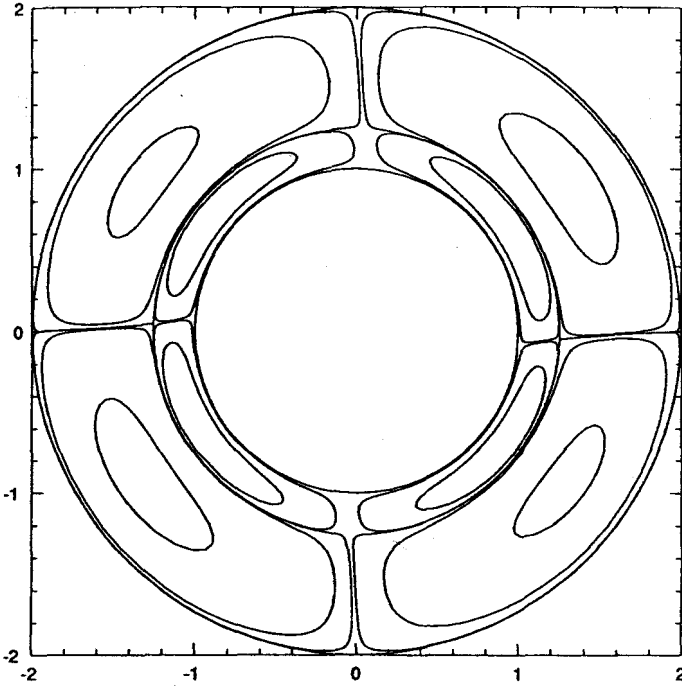


Fig. 4. The surfaces of constant adiabatic invariant for $\lambda = 2$, $|\Omega_1| = |\Omega_2|$ and the angle between Ω_1 and Ω_2 equal 5° .

adiabatic approximation is not valid because the periods of the unperturbed orbits are unbounded.

In figure 6a) we show the drift surfaces computed from (4.4) with $\Omega_1 = -\Omega_2$. The two cells in each quadrant have helicities of the *same* sign, and, away from $r = r_1$, the surfaces match the stream-surfaces of $\mathbf{u}^{(0)} + Re\mathbf{u}^{(1)}$ as given by (2.5), (3.15). In figure 6b) we show, qualitatively, the structure of the drift. The X-type stagnation points and the separatrices joining them make it possible to have a two-cell drift with the same sense of rotation in both cells.

However, the special surface $\Omega(r) = 0$ exists *only* when α is exactly zero. For any finite α we have $\Omega \neq 0$ everywhere and the periods of the unperturbed orbits are bounded. Hence, for any small α and sufficiently small Re the streamlines of $\mathbf{u}^{(0)} + Re\mathbf{u}^{(1)}$ are on the drift surfaces similar to those shown in figure 6. ² Then the fluid in the two cells is separated and does not mix.

² 'Sufficiently small' means such that the time-scale of $Re\mathbf{u}^{(1)}$ is everywhere small compared with $2\pi/|\Omega(r)|$.

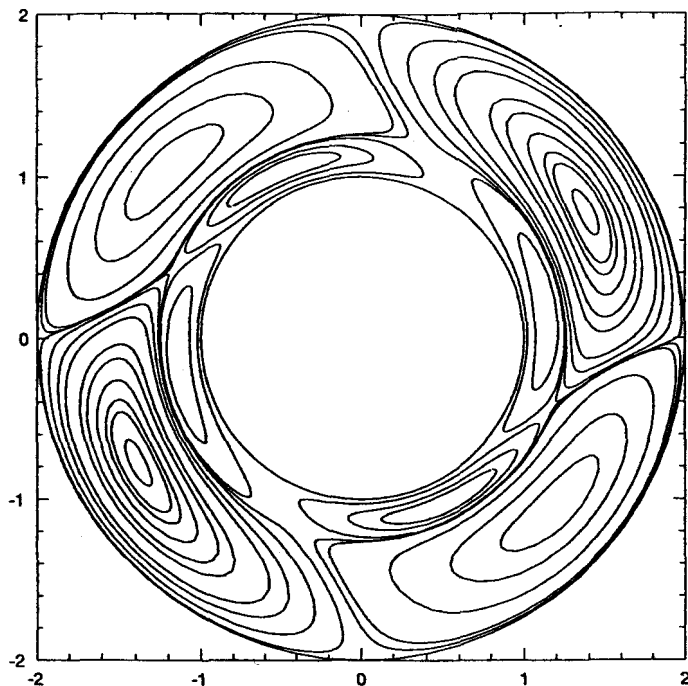


Fig. 5. The drift surfaces for $\Omega_1 = (1/\sqrt{2}, 0, 1/\sqrt{2})$, $\Omega_2 = (0, 0, 1)$.

If the (small) Reynolds number is fixed and we decrease α , then, in the limit $\alpha \rightarrow 0$ the drift surfaces tend to the limit shown in figure 6, but when α is too small the streamlines of $\mathbf{u}^{(0)} + Re\mathbf{u}^{(1)}$ begin to 'jump' across the surface $\Omega(r) = 0$ and they switch to a 'single-cell' pattern. This transition occurs at a critical value of $\alpha = \alpha_c(Re)$ which tends to zero when $Re \rightarrow 0$. Therefore, for small Re the change from a single-cell drift to a double-cell drift is 'almost discontinuous': the boundary between the two cells does not emerge from either wall but stays on the surface $\Omega(r) = 0$.

When ω_2/ω_1 is such that the axisymmetric flow has two cells then a small deflection creates a three-cell drift. In figure 7 we show the drift surfaces for $\Omega_2 = \hat{\mathbf{i}}_z$, $|\Omega_1| = 3.3$ and the angle between Ω_1 and Ω_2 equal 175° .

6. Transition to chaos

If the averaging procedure is valid in the entire domain, then, in the limit of $Re \rightarrow 0$, the surfaces of constant adiabatic invariant are identical with the stream-surfaces of $\mathbf{u}^{(0)} + Re\mathbf{u}^{(1)}$. For finite Re we obtain the Poincare sections of the streamlines by numerically solving the equations:

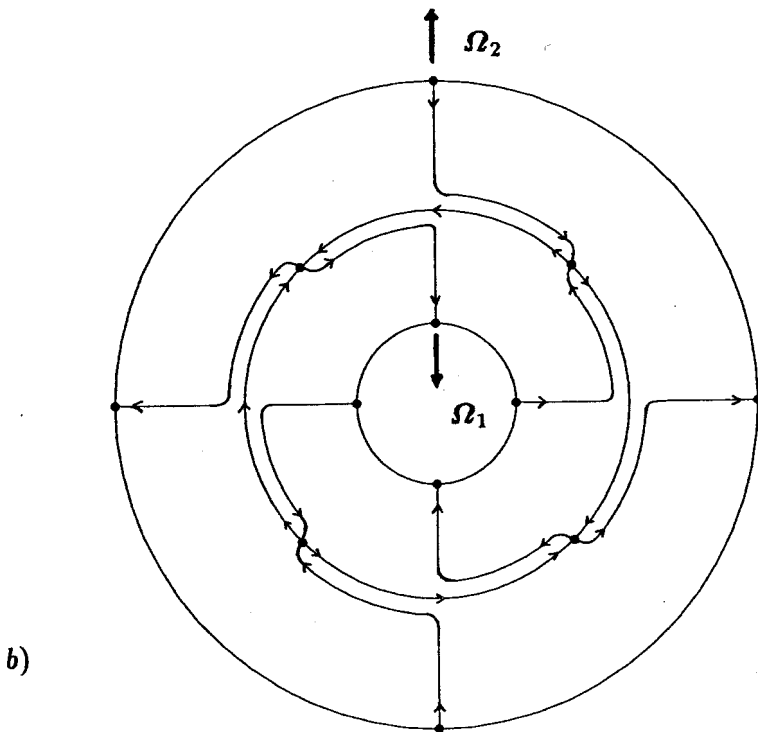
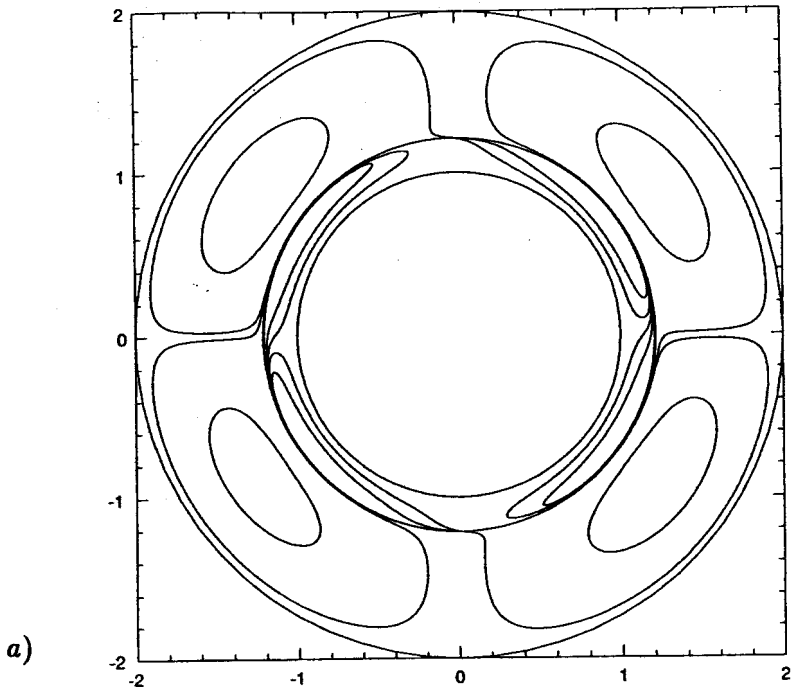


Fig. 6. (a) The drift surfaces (solutions of 4.4) for $\lambda = 2$, $\Omega_1 = -\Omega_2$.
 (b) The qualitative structure of a two-cell drift with the same sign of helicity in both cells

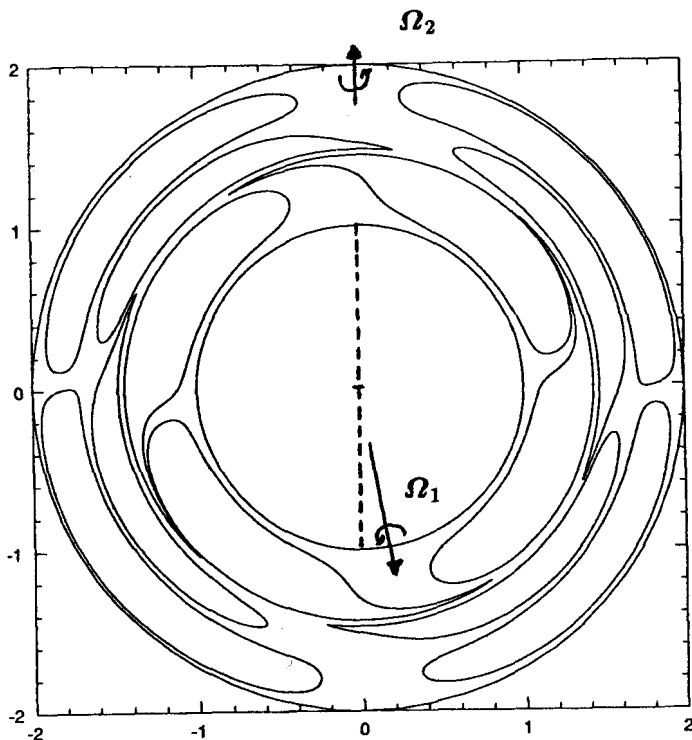


Fig. 7. The three-cell drift for $\lambda = 2$, $\Omega_2 = \hat{i}_z$, $|\Omega_1| = 3.3$ and the angle between Ω_1 and Ω_2 equals 175°

$$\frac{dx}{dt} = \mathbf{u}^{(0)} + Re\mathbf{u}^{(1)} \quad (6.1)$$

We find that the streamlines stay near the surfaces of constant adiabatic invariant for the Reynolds number as high as 10. In figure 8 we show the drift surfaces for $\Omega_1 = (\frac{2}{5}, 0, \frac{1}{5})$, $\Omega_2 = (0, 0, 1)$, and in figure 9 two streamlines of $\mathbf{u}^{(0)} + Re\mathbf{u}^{(1)}$ for $Re = 1, 10$. For $Re = 1$ the streamlines are practically indistinguishable from the adiabatic surfaces. When $Re = 10$ the inner streamline is still very close to a drift surface. The outer one, which is close to a separatrix, is 'out of focus', i.e. it generally follows an adiabatic surface but also has a significant chaotic transverse scatter. When the Reynolds number is further increased we observe, as might be expected, a transition to global chaos. In figure 10 we show the Poincaré section of a single streamline for $Re = 20$. The chaotic streamline penetrates most of the spherical annulus. Four islands can be seen near the elliptic stagnation points of the drift. The transverse chaotic scatter is smallest there and this region is the last to participate in global chaos.

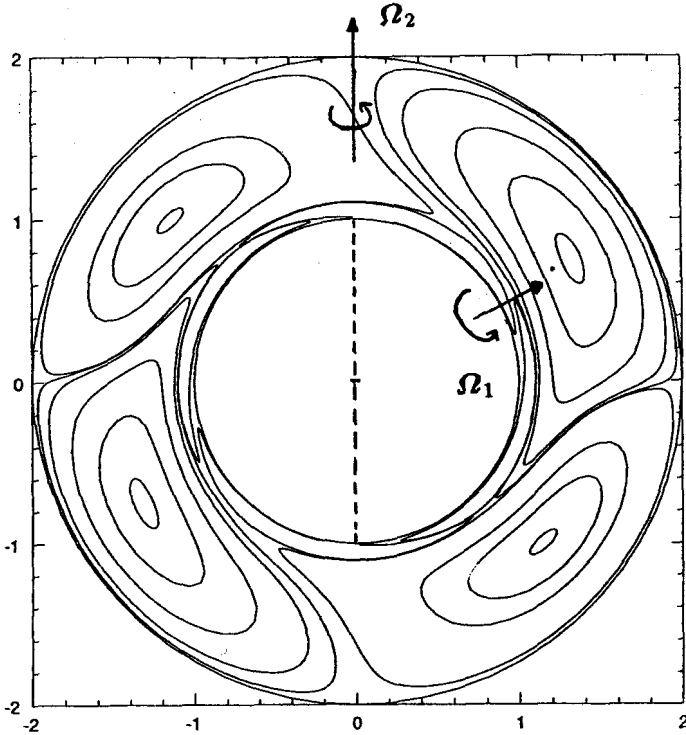


Fig. 8. The drift surfaces for $\lambda = 2$, $\Omega_1 = (\frac{2}{5}, 0, \frac{1}{5})$, $\Omega_2 = (0, 0, 1)$.

7. Conclusions

We have shown that the streamline pattern in the low Reynolds number flow between two rotating solid spheres can be explained in terms of an adiabatic invariant. The level surfaces of this invariant have to be computed numerically, but some important information about the topology of the flow, e.g. the number of drift cells and the positions of their boundaries, can be derived analytically. The Reynolds number is a parameter which can be controlled in a laboratory experiment and hence, the above analysis could, in principle, be verified experimentally.

We have also shown that the low Reynolds number flow obtained by adding the first order correction to the Stokes flow (i.e. $\mathbf{u}^{(0)} + Re\mathbf{u}^{(1)}$) has strongly chaotic streamlines for $Re \sim 20$. For such Re the first order approximation may still be valid, as it is, for example, in a two-dimensional flow around a solid cylinder. It is possible that in a spherical annulus, at $Re = 20$, higher order corrections must be added, but this is unlikely to change the chaotic nature of the flow.

The analysis of the drift surfaces in a weakly non-axisymmetric case en-

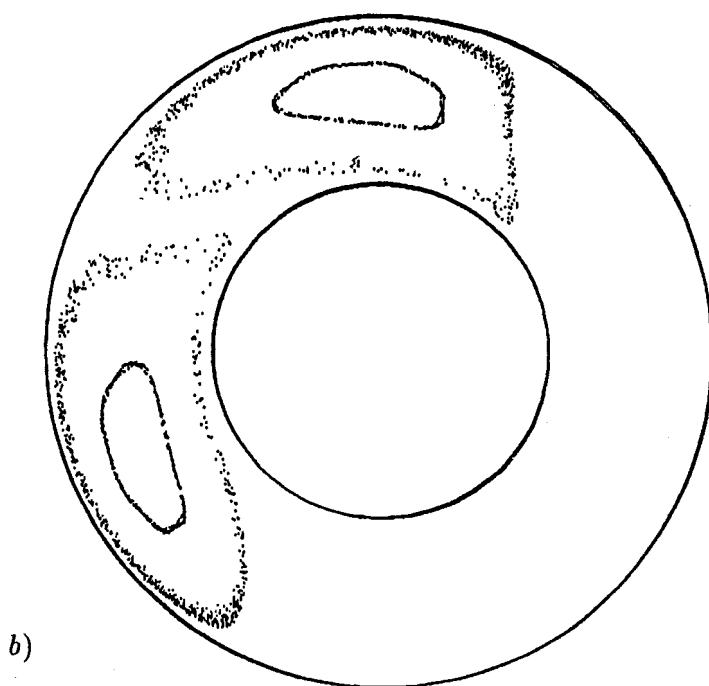
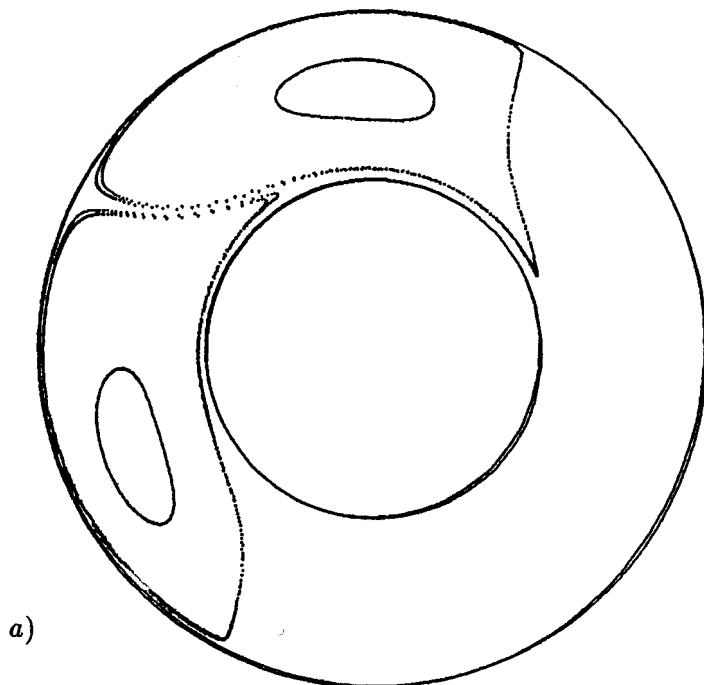


Fig. 9. The Poincaré sections of the two streamlines of $\mathbf{u}^{(0)} + Re\mathbf{u}^{(1)}$ with α , Ω_1 , Ω_2 as in fig. 8 and (a) $Re = 1$, (b) $Re = 10$.

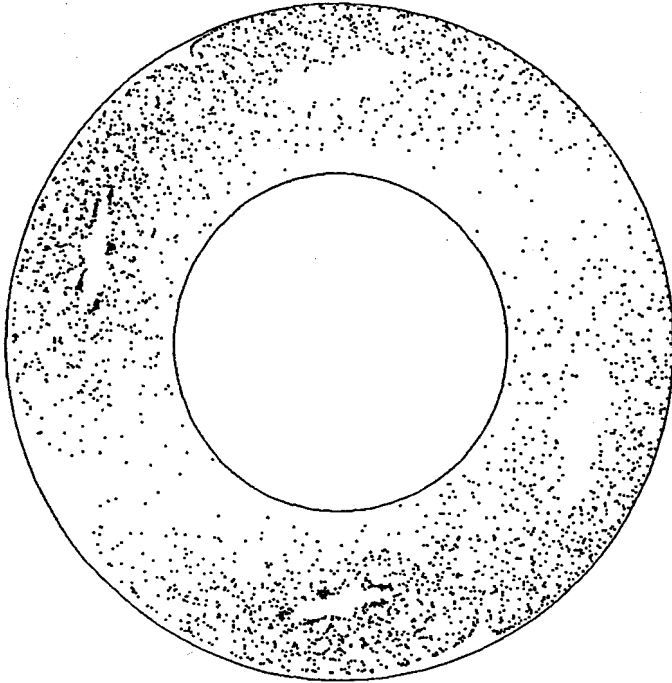


Fig. 10. The Poincaré section of a single streamline of $u^{(0)} + Reu^{(1)}$ with α , Ω_1 , Ω_2 as in fig.8 and $Re = 20$.

abled us to predict a qualitative change in the streamline topology in the case when $\Omega_1 \cdot \Omega_2 < 0$ and $\Omega_1 \wedge \Omega_2$ is small. The drift flow changes from the two-cell to one-cell pattern. This change is realised by the process of 'diffusion' of streamlines across the surface $f_1(r)\Omega_1 + (1 - f_1(r))\Omega_2 = 0$. A study of this (anomalous) 'diffusion' presents a challenging theoretical problem.

References

- BAJER, K., MOFFATT H.K. & NEX, F.H., 1990 Steady confined Stokes flows with chaotic streamlines. *Topological Fluid Mechanics*, Proceedings IUTAM Symposium, Cambridge, August 13-18, 1989, Eds: H.K. Moffatt & A. Tsinober, Cambridge University Press, 1990.
- BAJER, K., & MOFFATT H.K., 1990 On a class of steady confined Stokes flows with chaotic streamlines. *J. Fluid Mech.*, **212**, pp. 337-363.
- LANDAU, L.D., & LIFSHITZ, E.M., 1987 *Fluid Mechanics* (2nd Edn.), Pergamon Press.
- MOFFATT, H.K., 1991 Electromagnetic stirring. *Phys. Fluids A*, **3**(5), pp. 1336-1343.
- PROUDMAN, I., 1956 The almost rigid rotation of viscous fluid between concentric spheres. *J. Fluid Mech.*, **1**, pp. 505-516.
- STONE, H.A., NADIM, A., STROGATZ, S.H., 1991 Chaotic streamlines inside drops immersed in steady linear Stokes flows. *J. Fluid Mech.* (to appear)